The Effect of Cerium Precursor Agglomeration on the Synthesis of Ceria Particles and Its Influence on Shallow Trench Isolation Chemical Mechanical Polishing Performance

Japanese Journal of Applied Physics
Vol. 44, No. 12, 2005, pp. 8422–8426

The Effect of Cerium Precursor Agglomeration on the Synthesis of Ceria Particles and Its Influence on Shallow Trench Isolation Chemical Mechanical Polishing Performance

Dae-Hyeong KIM, Sang-Kyun KIM[1], Hyun-Goo KANG[2], Jea-Gun PARK[2] and Ungyu PAIK[1]*

KCTech, 271-14, Kyeruk-Ri, Miyang-Myon, Anseong-Si, Kyongki-Do, Korea
[1]*Department of Ceramic Engineering, Hanyang University, Seoul 133-791, Korea*
[2]*Nano-SOI Process Laboratory, Hanyang University, Seoul 133-791, Korea*

(Received July 11, 2005; accepted September 26, 2005; published December 8, 2005)

The level of agglomeration in the cerium precursor and its effect on the physicochemical properties of the synthesized ceria particles and how these properties influence shallow trench isolation chemical mechanical polishing (STI CMP) performance were investigated. Two different types of ceria particles were synthesized from cerium precursors of different degrees of agglomeration. The crystallinity and particle size distribution of the synthesized ceria particles were markedly different between these two types of particles. The ceria particles synthesized from agglomerated cerium precursors had a smaller crystallite size than the other particles due to the incomplete decarbonation reaction, which resulted in large agglomerations of particles. The different physical characteristics of the ceria particles resulted in remarkable discrepancies between the STI CMP performances of the ceria slurries, such as the oxide removal rate, the selectivity and the uniformity.
[DOI: 10.1143/JJAP.44.8422]

KEYWORDS: cerium precursor, agglomeration, calcination, ceria, STI CMP

1. Introduction

Chemical mechanical planarization (CMP) is a key process in contemporary ultra large scale integration (ULSI) fabrication. The shallow trench isolation (STI) process is one of the most crucial applications of CMP technologies and has replaced the local oxidation of silicon (LOCOS) method, because it significantly reduces the area required to isolate transistors, enhances the packing density, and offers the high degree of planarity that is necessary to meet stringent photolithography requirements. A ceria slurry is frequently used in STI CMP, because the ceria slurry, when compared with other abrasive slurries, offers improved selectivity for the planarization of the trench fill material while maintaining the polish stop layer at a uniform thickness.[1–5] The ceria slurry, however, has some critical disadvantages, including the many kinds of defects that are triggered by agglomeration, such as undesirable surface roughness and micro-scratches.[6–10] Furthermore, as target dimensions of the semiconductor devices decrease to below 90 nm, achieving high selectivity and good uniformity with large agglomerated slurry particles becomes more difficult. Therefore, it is necessary to minimize the agglomeration of particles in the slurry suspension and obtain a high selectivity and oxide removal rate.

Recently, many scientists have investigated the polishing mechanism of the SiO_2 film by ceria particles as well as the physicochemical properties of the ceria particles.[1,11–13] However, few studies have discussed the relationship between the characteristics of the cerium precursor and the physicochemical properties of the synthesized ceria particles, which significantly influence the STI CMP performance. The calcination process that transforms the cerium precursor to cerium oxide consists of a five-step mechanism which includes the mass-transfer of the reacting agent (oxygen) from the bulk atmosphere to the periphery of the carbonate, its diffusion through the carbonate pores, the adsorption of the reactant, the reaction with cerium carbonate, and finally the desorption of the reaction by-product (carbon dioxide).[14,15] Thus, it is expected that the morphology of the starting precursor plays an important role in the de-carbonation reaction, since the ability of the reactant and product to diffuse into and out of the pores affects the de-carbonation reactivity at the reaction site and eventually CMP performance.[13,14] Consequently, the calcination process as a function of the morphology of the cerium precursor and the physicochemical properties of the synthesized ceria particle should be thoroughly understood to yield good STI CMP performances.

In this study, we prepared two different ceria particles from cerium carbonate precursors that had different degrees of agglomeration. The effect of the precursor's characteristics on the physicochemical properties of the synthesized ceria particles and their influence on later STI CMP performance were investigated with the aim of improving the removal selectivity and uniformity, and reducing the scratches on the wafer surface.

2. Experimental Procedure

Two kinds of cerium carbonate (Jun Tai Rare Earth, Shanghai, China) were used for the synthesis of the ceria particles. In order to prepare two different types of cerium precursors, the starting solutions were prepared with and without poly(ethylene glycol) (PEG, $M_W = 14000$, Aldrich, U.S.A.) using the wet precipitation method. The morphology and the particle sizes of the two different kinds of cerium carbonates were compared using the scanning electron microscopy (SEM; S-900, Hitachi, Japan) images shown in Fig. 1(a). The cerium precursor prepared with PEG, sample A, has a thinly dispersed and plate-like structure, while sample B, prepared without PEG, shows a spherically agglomerated structure. Ceria powders were synthesized by the solid-state displacement reaction method, in which the two kinds of cerium carbonates mentioned above were employed as starting materials. The SEM images of these particles are shown in Fig. 1(b). The morphology of the synthesized ceria particles was similar to both cerium precursors. After calcination, ceria powders underwent

*E-mail address: upaik@hanyang.ac.kr

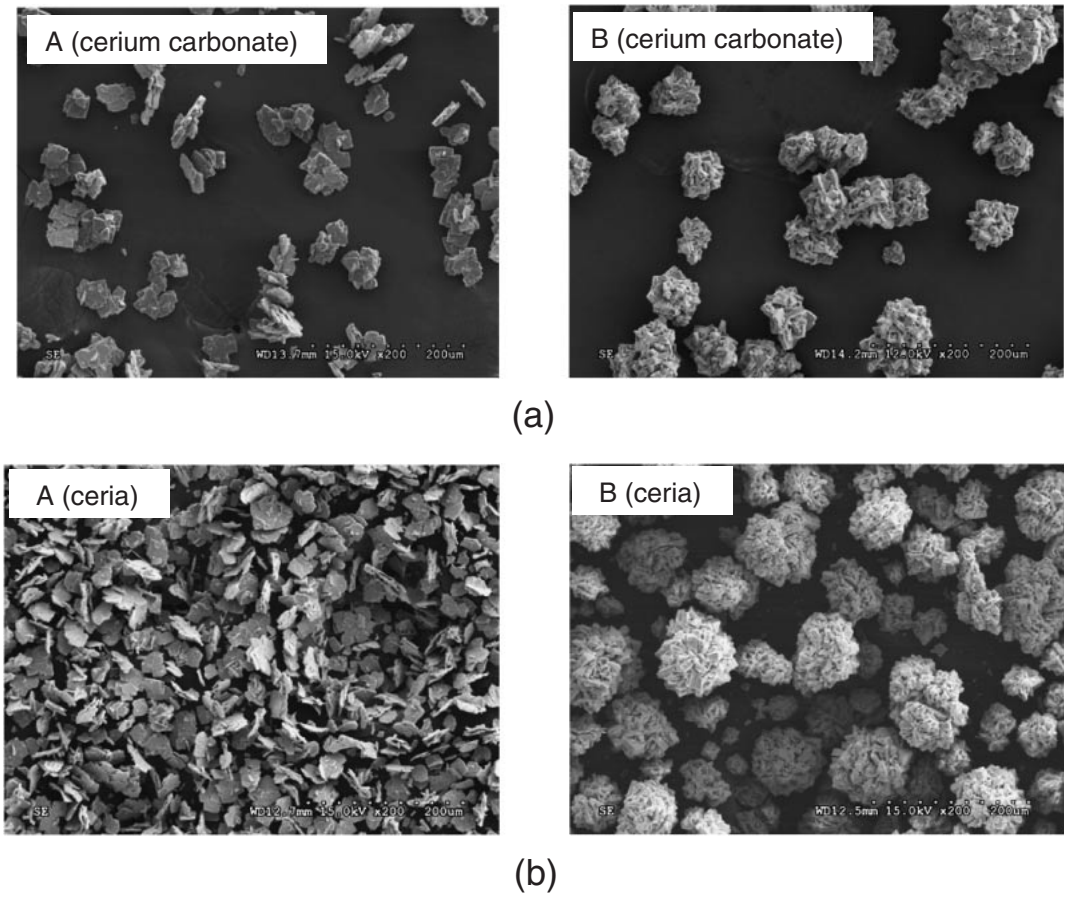

Fig. 1. Particle morphology as shown by SEM images: (a) cerium carbonate and (b) synthesized ceria particles.

mechanical milling for several hours to reduce their size to the target and to disperse the particles in the aqueous medium after mixing with de-ionized water and a commercially available anionic acrylic polymer dispersant. The solid content of the slurry was controlled at a weight fraction of 5%.

The crystallite size of the ceria particles was measured by X-ray diffraction (XRD; RINT/DMAX-2500, Rigaku, Japan), and calculated from the Debye–Scherer equation. In addition, the specific surface area of powders was estimated using the Brunauer–Emmett–Teller (BET) method (ASAP 2010, Micromeritics, U.S.A.), and the powder density was measured by using a pycnometer (Accupyc 1330, Micromeritics, U.S.A.). The grain size was also observed using transmission electron microscopy (TEM; JEM-2010, JEOL, Japan). In order to investigate the agglomeration tendencies of the ceria particles in an aqueous medium, a particle size analyzer was used (LA-910, HORIBA, Japan) that was equipped with an ultrasonic generator, which is capable of breaking agglomerated particles using cavitation energy. Particle sizes were measured both with and without ultrasonic treatment, and the difference between the particle size measurements was calculated as a basis for judging the degree of agglomeration.[16] In order to quantify the degree of agglomeration, the following quantities were defined:

$$\begin{aligned} \mathrm{dD1} = {} & \text{D1 without ultrasonic treatment} \\ & - \text{D1 with ultrasonic treatment} \end{aligned}$$

$$\begin{aligned} \mathrm{dD15} = {} & \text{D15 without ultrasonic treatment} \\ & - \text{D15 with ultrasonic treatment} \end{aligned}$$

$$\begin{aligned} \mathrm{dD50} = {} & \text{D50 without ultrasonic treatment} \\ & - \text{D50 with ultrasonic treatment} \end{aligned}$$

in which D1, D15, and D50 denote the particle size of 1, 15, and 50% from the largest particle size found in the particle size distribution, respectively.

The field evaluation of CMP was accomplished using the two types of ceria slurries synthesized in this study. In the evaluation of CMP, an 8″ wafer CMP tool (6EC, Strasbaugh, U.S.A.) was used. The polishing pad was a grooved IC1000/SubaIV (Rodel, U.S.A.). After CMP, the wafers were cleaned using an APM solution ($NH_4OH : H_2O_2 : H_2O = 1 : 1 : 10$) at 80°C to eliminate residual particles. The film thickness was measured using a Nanospec 180 (Nanometrics, CA, U.S.A.) to calculate removal rates. For this experiment, the within wafer non-uniformity (WIWNU) was defined as the standard deviation of the remaining thickness divided by the average of the remaining thickness after CMP. Scratch counts on the PETEOS film were measured using a Surfscan SP1 (KLA-Tencor, U.S.A.). The polishing test conditions are shown in Table I.

3. Results and Discussion

The physicochemical properties of the synthesized ceria particles were investigated as a function of the morphology of the cerium precursor and the diffusion resistance of the

Table I. CMP conditions.

Machine model	Strasbaugh 6EC
Pad	IC1000/Suba IV k-groove
Table speed (rpm)	70
Spindle speed (rpm)	70
Down force (psi)	4
Back pressure (psi)	0
Time (s)	30
Flow rate (ml/min)	100

oxygen and carbon dioxide. Ceria powders were synthesized by the solid-state displacement reaction method in the temperature range of 700–900°C, for which two kinds of cerium carbonates were employed as starting materials, including one that was thin and plate-like and one that was spherically agglomerated. As shown in Fig. 1, the morphology of the synthesized ceria particles was similar to that of the cerium precursors which demonstrated that the morphology of carbonate precursor was maintained through the decarbonation reaction. When considering the decarbonation reaction mechanism of the carbonate precursor in which the mass-transfer of oxygen and carbon dioxide are important factors determining the reaction rate of decarbonation,[14] and the unchanged morphology of the precursor carbonate after calcination, it is expected that the morphology of the cerium precursor has a significant influence on the physicochemical properties of the synthesized ceria particles. Figure 2 shows the BET surface area and the density of the ceria powders versus the grain size that was calculated from the XRD results. The surface area and density of samples A and B—whose grain sizes were controlled at three sizes, 25, 30, and 47 nm—were compared. Grain size is an indication of crystallinity; as it increased, the surface area decreased and the density increased. These results were in general agreement with results reported previously.[13] This phenomenon is due to the grain growth as a function of temperature during the calcination process, in which atomic diffusion causes the wetting of the grain boundaries of adjacent grains. With further atomic diffusion, the crystallinity (and thus the grain size of the particle) increased, which resulted in a higher

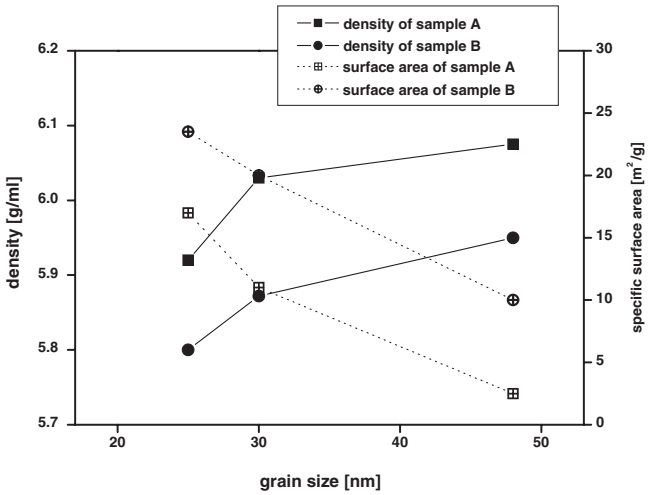

Fig. 2. Specific surface area and density of samples A and B with regard to grain size calculated using XRD data.

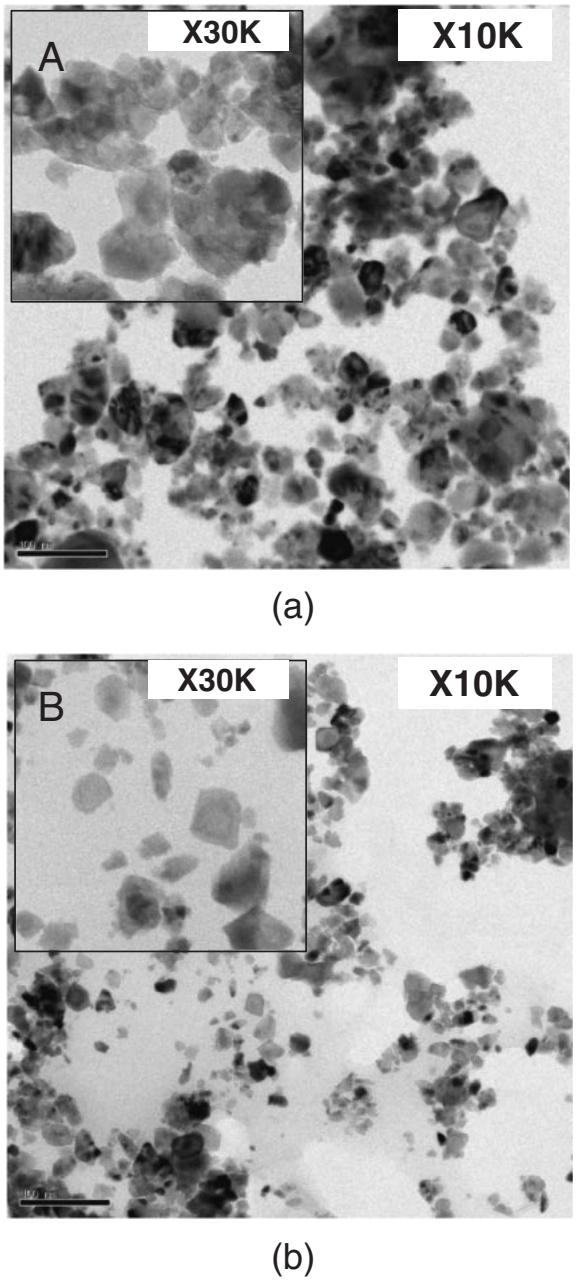

Fig. 3. TEM images of cerium oxide: (a) sample A and (b) sample B.

density and smaller surface area. As shown in Fig. 2, however, sample B had a larger surface area and was less dense than sample A, which indicated a lower crystallinity in sample B, even when the XRD grain size was the same. In addition, as shown in Fig. 3, TEM images of the ceria particles after mechanical milling confirm that there was less crystal growth in sample B, in which the agglomerated precursor was used. The grain size calculated from the XRD data for each TEM sample was 30 nm.

This phenomenon can be attributed to incomplete calcination, which resulted in less crystal growth at the center of the spherically agglomerated carbonate in the case of sample B. According to several previous reports, the reactivity of the calcination process depends heavily on the physical and structural properties of the precursor. The shrinking core model explains the calcination process of the carbonate precursor.[14,15,17,18] In this model, the calcination

reaction takes place at the outer surface of the particle at the initial stage of the reaction. As the reaction proceeds, the exterior surface of the particle is covered with reacted product, cerium oxide. The un-reacted remaining carbonate core shrinks into the interior region of the particle. Particle size remains constant while the diameter of the un-reacted core decreases with time. However, with sufficient calcination, this un-reacted core will also undergo the de-carbonation reaction. In the case of severely agglomerated precursors, oxygen diffusion resistance slows the de-carbonation reaction at the reaction site, and the diffusion of the carbon dioxide retards the production of carbon dioxide due to the accumulation of the reaction product. This phenomenon prevents complete calcination and disturbs the decarbonation reaction of the agglomerated precursor, resulting in less crystallinity, especially in the center of these agglomerated precursors.

In order to investigate the degree of calcination of the ceria particles, the average grain size was calculated from XRD data. In the XRD method, the X-ray penetrates only ten micrometers into the powder surface, diffracting only near the surface relative to the larger diameter of the agglomerated precursor.[19] Therefore, the core part of the agglomerated cerium oxide cannot be measured with XRD alone after calcination. By using mechanical milling, however, the core part of the particles could be exposed. The average grain size of the particles before and after mechanical milling are shown in Table II. Even though the initial powder grain size of both samples that were calculated by the Debye–Scherer equation were near 29.7 nm, the grain sizes of the particles after mechanical milling became 28.7 and 22.6 nm for samples A and B, respectively. The crystallite size of sample B, which was calcined from agglomerated cerium precursors, was extensively reduced by the mechanical crushing, while the crystallite sizes in the slurry prepared from non-agglomerated cerium precursor were only slightly altered. These results confirmed that in sample B, the grains with less crystallinity were at the core of the agglomerated powder and agreed with the BET and density data, which denoted incomplete and inefficient calcination of the ceria particles at the center of the agglomerated precursors.

Figure 4 and Table III compare the degree of agglomeration between the ceria slurries. For each sample, particle agglomeration was quantified by using particle sizes with and without ultrasonic treatment. The particle sizes of both samples after the ultrasonic treatment were near 250 nm. For abrasive particles in the slurry suspension that were more agglomerated, the particle sizes after the ultrasonic treatment decreased more, resulting in large difference between the particle sizes before and after the ultrasonic treatment. More than any other value, the dD1 value significantly reflects the extent of agglomeration and scratching, since it is calculated with the particle size of the tailing agglomerated part. As shown in Fig. 4 and Table III, incompletely calcined ceria particles were more agglomerated and this agglomeration possibly induced the micro-scratches.[6–10] As shown in Fig. 3, the incompletely calcined ceria slurry had much smaller particles; those small particles were likely to have originated from the inner part of the agglomerated particle. Since these small particles had a large surface area and significantly high surface energy, the agglomeration of the particles occurred readily in the slurry. Such agglomeration reduced the surface potential and stabilized the slurry system consisting of numerous small particles.

The results of the CMP evaluation with the two different ceria slurries are shown in Fig. 5. As shown in Fig. 5(a), the slurry made with the agglomerated cerium precursor had a lower oxide removal rate, which resulted in poor oxide to nitride selectivity. In STI CMP, ceria particles penetrated the viscous layer on the oxide or nitride layer, reacted with the

Table II. Average grain size before and after size reduction by mechanical milling.

Sample	Average grain size (nm)		Decrement (nm)
	before milling	after milling	
A	29.8	28.7	1.1
B	29.6	22.6	7

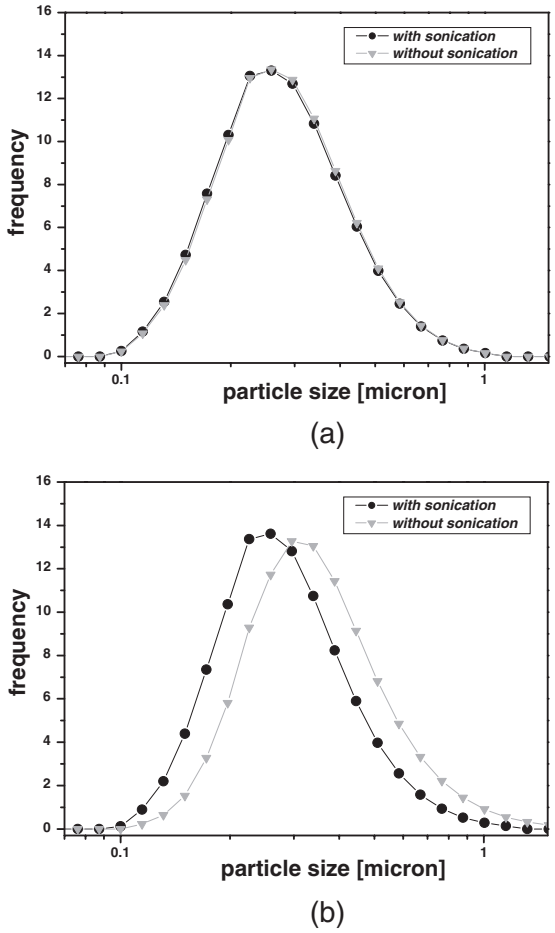

Fig. 4. Particle sizes with and without ultrasonic treatment: (a) sample A and (b) sample B.

Table III. Size differences between samples with and without ultrasonic treatment.

Sample	dD1 (nm)	dD15 (nm)	dD50 (nm)
A	4	3	3
B	254	101	57

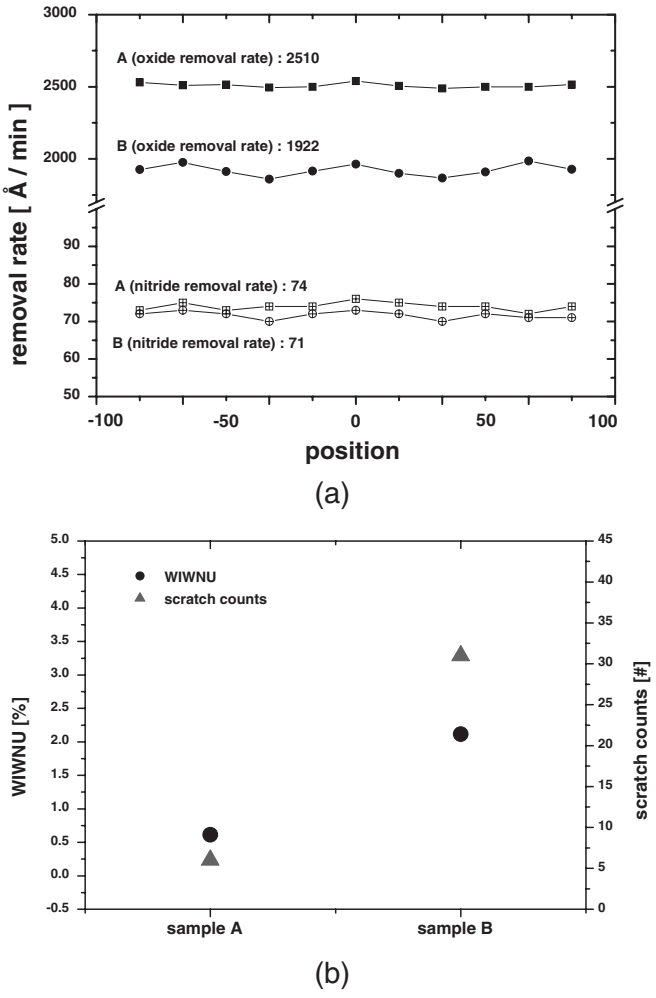

Fig. 5. Results of CMP field evaluation: (a) average removal rate and (b) WIWNU and scratch counts on the oxide wafer.

hydrated surface to form covalent bonds like Ce–O–Si, and then pulled off the lumps of oxide and nitride.[20] Therefore, as the crystal size decreased due to incomplete calcination and hindered grain growth, the possibility of penetration into the viscous layer was decreased and translated into a lower oxide removal rate. However, the viscous layer on the nitride layer was thicker than that on the oxide layer, too thick for a difference in crystal sizes to be detected in nitride removal rate.[21,22] Thus, the nitride removal rate did not effectively demonstrate the great difference between samples A and B, which led to poor selectivity in the case of the agglomerated precursor. The WIWNU and scratch counts after CMP are shown in Fig. 5(b). The WIWNU of sample B was larger than that of sample A. Since sample B had more agglomerated particles and was thus more viscous than sample A, the slurry suspension of sample B hardly covered the whole wafer surface during CMP.[23] This result caused a discrepancy between the removal rate at the center of the wafer and at the edge of the wafer surface. Furthermore, the scratch counts of sample B were 5 times larger than that of sample A. During CMP, the agglomerated particles stuck on the wafer surface due to the small interactive forces between the abrasive and wafer surface.[24] These particles induced the surface scratches on the wafer due to the compressive and shear forces between the wafer and pad. Therefore, agglomerated particles were found to be a major cause of the scratches in the CMP process. Consequently, the minimization of particle agglomeration using a non-agglomerated cerium precursor was found to be important for uniform and complete crystal growth of the ceria particle, ensuring not only good dispersion of the ceria slurry but also a high removal selectivity with fewer micro-scratches.

4. Conclusions

In this study, we investigated the effect of agglomerated cerium carbonate on the physicochemical properties of the synthesized ceria particles and the eventual performance of STI CMP. The degree of agglomeration of the cerium precursor was a major factor in the success or failure of the decarbonation calcination process. When the cerium precursors were agglomerated, the calcination process was incomplete in the core part of the particle due to the diffusion resistance of oxygen. This incomplete calcination led to a poor dispersion of the ceria particles. Therefore, the incomplete crystal growth of the ceria particles resulted in a low polishing rate and selectivity with numerous scratches on the wafer surface. Consequently, limiting the agglomeration of the cerium precursor before calcination is an important factor for good performance of STI CMP.

1) H. Nojo, M. Kodera and R. Nakata: Proc. IEEE, San Francisco, CA, 1996, p. 349.
2) K. Hirai, H. Ohtsuki, T. Ashizawa and Y. Kurata: Hitachi Chemical Tech. Rep., 2000, No. 35, p. 17.
3) Y. Tateyama, T. Hirano, T. Ono, N. Miyashita and T. Yoda: Proc. Int. Symp. Chemical Mechanical Planarization IV, Phoenix, 2000, p. 297.
4) T. Katoh, H. G. Kang, U. Paik and J. G. Park: Jpn. J. Appl. Phys. **42** (2003) 1150.
5) J. P. Kim, U. Paik and J. G. Park: J. Korean Phys. Soc. **39** (2000) 197.
6) T. Detzel, S. Hosali, A. Sethuraman, J. F. Wang and L. Cook: Proc. CMP-MIC Conf., 1997, p. 202.
7) G. B. Basim, J. J. Adler, U. Mahajan, R. K. Singh and B. M. Moudgil: J. Electrochem. Soc. **147** (2000) 3523.
8) R. K. Singh, S. M. Lee, K. S. Choi, G. B. Basim, W. Choi, Z. Chen and B. M. Moudgil: MRS Bull. (Oct., 2002) 752.
9) T. L. Neo, E. S. Y. Shang and C. M. Chong: Proc. Int. Symp. Semiconductor Manufacturing, San Jose, CA, 2001, p. 321.
10) Y. J. Seo, G. U. Kim and W. S. Lee: Microelectron. Eng. **71** (2004) 209.
11) S. H. Lee, Z. Lu, S. V. Babu and E. Matijević: J. Mater. Res. **17** (2002) 2744.
12) T. Hoshino, Y. Kurata, Y. Terasaki and K. Susa: J. Non-Cryst. Solids **283** (2001) 129.
13) S. K. Kim, P. W. Yoon, U. Paik, T. Katoh and J. G. Park: Jpn. J. Appl. Phys. **43** (2004) 7427.
14) O. Levenspiel: *Chemical Reaction Engineering* (Wiely, New York, 1999) 3rd ed., Chap. 18, p. 378.
15) C. H. Lu and H. C. Wang: Mater. Sci. Eng. B **90** (2002) 138.
16) B. Pacaud, T. K. Doy, Y. Sasakawa and E. Rohart: unpublished.
17) I. Ar and G. Dogu: Chem. Eng. J. **83** (2001) 131.
18) G. Dogu: Chem. Eng. J. **21** (1981) 213.
19) P. Shankar, D. Sundararaman and V. S. Raghunathan: Mater. Lett. **14** (1992) 67.
20) F. Sadi, D. Duprez, F. Gérard and A. Miloudi: J. Catal. **213** (2003) 226.
21) J. G. Park, T. Katoh, W. M. Lee, H. Jeon and U. Paik: Jpn. J. Appl. Phys. **42** (2003) 5420.
22) H. G. Kang, T. Katoh, M. Y. Lee, H. S. Park, U. Paik and J. G. Park: Jpn. J. Appl. Phys. **43** (2004) L1060.
23) S. K. Kim, S. K. Lee, U. Paik and T. Katoh: J. Mater. Res. **18** (2003) 2163.
24) C. F. Yeh, C. W. Hsiao and W. S. Lee: Appl. Surf. Sci. **216** (2003) 46.